AIAA 2013-4034

# Slit FEEP Thruster Performance with Ionic Liquid Propellant

Salvo Marcuccio[1]
*University of Pisa, Italy 56122*

Nicola Giusti[2] and Pierpaolo Pergola[3]
*Alta SpA, Pisa, Italy 56121*

**By replacing the liquid metal propellant with a ionic liquid, it is possible to develop a new, simplified FEEP system that combines most of the heritage and the advantages of the linear slit geometry with the easy of handling and operation of a more benign propellant. In view of the development of such Ionic Liquid FEEP thruster (IL-FEEP), an internal development activity is underway at Alta, aimed at the design and testing of an innovative linear slit thruster derived from the cesium experience. This paper presents the results of recent experimental campaigns aimed at assessing the performance of linear slit FEEP emitters fed with a ionic liquid propellant. For the first time, beam composition was evaluated using a time-of-flight mass spectrometry technique, allowing for a reliable estimate of the thruster's specific impulse.**



## I. Introduction

FIELD Emission Electric Propulsion (FEEP) is suited for very low thrust (1μN-1mN), high accuracy applications, with very high specific impulse, reduced system mass and volume and high accuracy at very low thrust levels. The thruster consists of a ionic source (emitter) with a micrometer sized, elongated slit of several mm, where a meniscus of a conductive liquid is ionized and accelerated by a very high electric field. The electric field causes instabilities on the liquid surface that generate a series of discrete ion emission sites along the meniscus, with as much as hundreds of individual sources. Such arrangement is called a "linear slit FEEP thruster", to distinguish it from simpler devices where emission takes place from a single, point-like site at the tip of a needle or at the end of a capillary.

Contrary to other electric thrusters, FEEP produces no plasma and has therefore no high temperature parts, allowing for easy integration with the spacecraft. The currently available FEEP system was designed to meet the very stringent requirements of the LISA Pathfinder mission and, in general, of fundamental physics space missions[1]. In this "classical" configuration the FEEP emitter is fed with cesium or, possibly, with other liquid metals. Cesium is usually preferred due to its low melting point (29 °C), low ionization potential and high atomic mass, which result in excellent propulsive performance. This choice, however, causes the present FEEP system to be rather complex and expensive, due to the very difficult handling of cesium, so that its use is justified only when very accurate and controllable thrust is required. However, many features of FEEP (high specific impulse, low volume, room temperature operation, long lifetime and unlimited re-ignition capability) are attractive for a wide range of applications, and are specially interesting for advanced small satellites. Fortunately, the FEEP emitter lends itself to operation with more benign propellants, such as ionic liquids (IL), although at a cost in terms of specific impulse. It is therefore possible to design and build a simplified, lower cost version of the FEEP thruster, well suited to most small satellite applications[2]. Development of such a simplified, IL-fed FEEP system is underway at Alta since a few years in the frame of projects funded by ESA and by the European Commission FP7 programme[3].

Promising results obtained using an experimental emitter made of glass were reported elsewhere[4]. Hereafter, we report on recent test campaigns carried out on a new generation stainless steel emitter. The main goal of the tests

[1] Associate Professor, Aerospace Division, Dept. of Civil and Industrial Engineering, Via Caruso 8, 56121 Pisa, Italy; Senior Member AIAA - s.marcuccio@ing.unipi.it
[2] Senior Researcher, Via A. Gherardesca 5, Ospedaletto, 56121 Pisa, Italy - n.giusti@alta-space.com
[3] Programme Manager, Via A. Gherardesca 5, Ospedaletto, 56121 Pisa, Italy - p.pergola@alta-space.com

were to assess the linear slit IL-FEEP behaviour and to identify the composition of the ejected beam of particles, so to be able to assess the thruster's specific impulse. In pure ionic regime, specific impulse is at its highest; on the contrary, large amounts of droplets in the beam (ion-droplets mixed regime) determine lower specific impulses, with corresponding higher thrust. Investigation of beam composition was performed by means of the Time-of-Flight (ToF) technique, using simple targets in the first test campaign and a specific detector in the second.

## II. Test Setup

### A. Vacuum facilities

The test campaigns were carried out in two different vacuum facilities:

- a cylindrical chamber with an inner diameter of 0.6 m and a length of 1.5 m (Fig. 1) for the first test campaign;
- a cylindrical chamber with an inner diameter of 0.5 m and a length of 1.0 m (Fig. 2) for the second test campaign.

The two chambers are equipped with similar vacuum pumping systems, both composed of a rotary pump (120 l/min pumping speed) for low vacuum ($10^{-2}$ mbar) and a turbo-molecular pump (500 l/sec) for high and ultra-high vacuum ($10^{-8}$ mbar). The small volume difference between the two facilities did not significantly affect the IL-FEEP thruster operation. The ultimate vacuum maintained with thruster firing was $10^{-6}$ mbar.

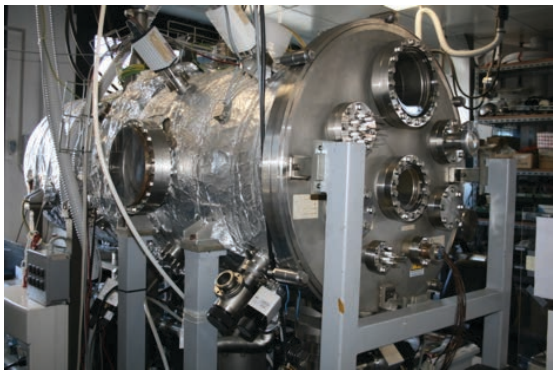

**Fig. 1 Test facility, first campaign.**

**Fig. 2 Test facility, second campaign.**

During both tests, all the relevant data were collected by means of a common acquisition system:

- analogue signals (vacuum chamber pressure, temperature values and thruster electrical parameters) and digital signals for facility automation were managed with a distributed I/O system operating at 1 Hz;
- beam scan measurements were acquired by means of a National Instruments PCI 6036e DAQ board (maximum sample rate of 200 kS/s);
- ToF measurements were taken with a Tektronix DPO4104B oscilloscope (maximum sample rate 5 GS/s).

### B. Thruster assembly

The design of the emitter units used for the test campaign with the ionic liquids is based on that of the cesium FEEP thruster. The emitter is manufactured in Inconel X750. It is composed of two half emitters, male and female, with the female half-emitter equipped with a vacuum-deposited, 1.5 μm thick layer of nickel. The deposition is shaped so as to realize the propellant duct when the two half-emitters are coupled. The effective portion of the linear slit is 8 mm in length. Pre-test handling of the emitter followed the strict quality control procedures developed for the cesium FEEP flight program and was carried out in the ISO5 clean room available at Alta's premises. Fig. 3 shows the emitter during a leaktightness test.

The thruster unit shield is a grounded box of stainless steel (Fig. 4). The case encloses completely the two electrodes leaving only an elliptic window in front of the thruster slit. Two additional windows, one on the right side and one on the top are left for the visual observation of the emitter during tests. The same case was used in both test campaigns. During thruster operation the emitter temperature was monitored by a fiber optic temperature sensor (FISO Technologies Inc.) placed on the emitter.

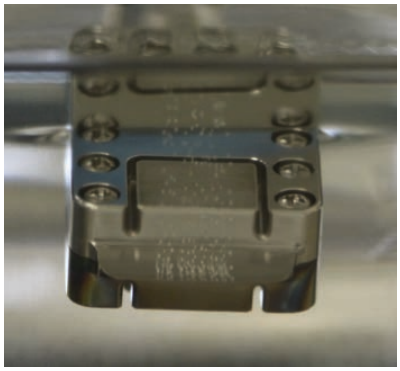

**Fig. 3 The FEEP emitter**

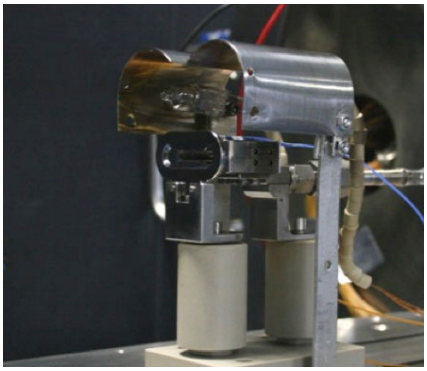

**Fig. 4 Thruster assembly**



### C. Propellant feed system

The propellant used in both test campaigns is 1-Ethyl-3-methylimidazolium tetrafluoroborate (EMI-BF4). The main properties of the propellant are:

| | |
|---|---|
| CAS number: 143314-16-3 | melting point: 15 °C |
| empirical formula (Hill Notation): C6H11BF4N2 | density: 1218 kg/m$^3$ |
| molecular weight: 197.97 | electric conductivity: 1.4 S/m |
| anion mass: 86.77 amu | surface tension: 0.0452 N/m |
| cation mass: 111.200 amu | viscosity: 0.038 Pa·s |

The propellant supply system consists of the feeding system, i.e. the propellant reservoir and ducts, and the pouring system, designed to refurbish the propellant consumed during operation. Most of the feeding system components are made of Pyrex glass, to allow for the visibility of the propellant head.

### D. High voltage power supply

In both test campaigns the positive or negative voltage was supplied to the emitter and the accelerator was grounded. Two different thruster power supply units were used for the two test campaigns. In test No. 1, a commercial high voltage supply was used (FuG HCP 140-12500), previously used during the cesium FEEP development programme. It operates in the voltage range 0 - 12.5 kV and current range 0 - 10 mA, allowing for a switching frequency between positive and negative polarity of the order of 0.1 Hz.

For the second test campaign, a dedicated power supply unit was developed with the primary goal of increasing the thruster voltage switching frequency. The power supply is based on a commercial DC/DC converter by EMCO, providing 0 to 10 kV of output voltage and up to 1 mA output current. Two EMCO modules are used, together with two high frequency, high voltage, military grade Reed relays.

### E. Beam scanning system

Scanning of the beam was performed with two single filament electrostatic probes moving inside the beam by means of two stepper motors (Fig. 5).

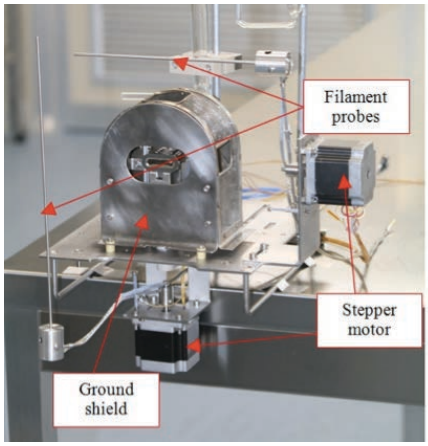


**Fig. 5 Filament probes for ion beam scanning.**

The wire probes are 120 mm in length and 2 mm in diameter. Both the vertical and the horizontal beam scans are performed by taking 32 measures in the two planes and each measure is computed as the mean of one thousand samples, acquired at a total sample rate of 200 kS/s. The divergence angles are computed so that they include the 97.5% of the beam current integral.

The beam scan system was used only during the first test campaign. During the second test campaign, the thruster was run always in high frequency alternate polarity, so that beam scanning was impossible. The same holds also for the I-V characteristics, that have been recorded only during the first test campaign.

### F. Time-of-Flight system

The basic principle behind the ToF method consists in measuring the time required for a charged particle to traverse a certain distance in a region free of external fields. The travel time allows for the computation of the particle's velocity, i.e.:

$$v = 2\,[(q/m)V_e\,]^{0.5}$$

where $V_e$ is the ion source potential and $q/m$ is the charge per unit mass of the particle.

The simplest way to perform ToF measurements is to suddenly remove the thruster voltage and to collect the emitted charged particles by means of a metallic target. The time variation of the collected current gives the travel time of the different beam species. Assuming that the beam is composed of singly charged ions and particles only, their mass can be inferred. The expected magnitude of the beam current integral is few microamps and, with a 1 m path (such as in our experimental arrangement), the shortest expected travel time is about $10^{-5}$ s. As a consequence, in the experimental setup a suitable high voltage switch with a very fast response is needed. The model used in our setup is a fast high voltage transistor switch Belhke HTS 201 G/03-GSM, with a turn-on/turn-off transient time of less than 10 ns.

In the first test campaign two simple metallic probes are used to collect the current:

- ToF1, a metallic wire placed in vertical position at the centre of the chamber (distance between the emitter tip and the probe: 600 mm),
- ToF2, a metallic target disk placed at the end of the chamber (distance between the emitter tip and the probe: 1300 mm).

In front of the metallic target disk two grids were placed to suppress the secondary electron emission: the first grid was at ground potential, the second one at - 90 V (Fig. 6).

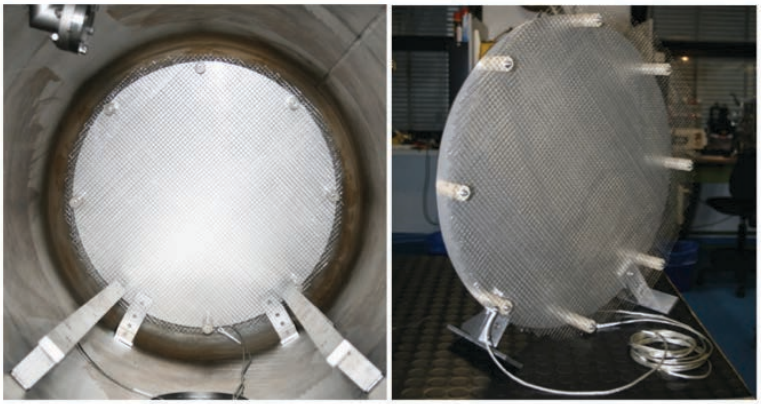

**Fig. 6 Target mounted in the vacuum chamber (left) and before integration (right).**

The beam current collected by the probes is in the range of few microamps and the noise induced from capacitive coupling affects significantly the measurements. For this reason, during the second test campaign the wire and target disk were replaced by a commercial electron multiplier, namely a 18 mm Dual Microchannel Plate (MCP) detector by Jordan TOF products, Inc., with a gain of about $10^6$ and sub-nanosecond rise time (Fig. 7).

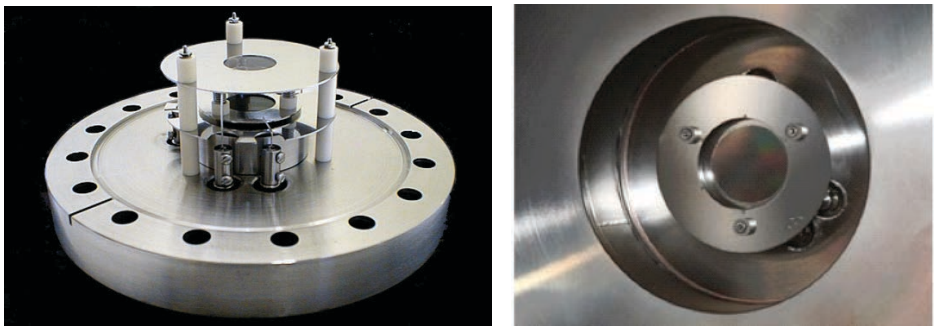

**Fig. 7 18 mm Dual Microchannel Plate Detector (Jordan TOF Product, Inc.)**

The MCP detector, when not used, was covered with a metallic shield to preserve the lifetime of the active surface. The shield also worked as target for emission current detection. The MCP detector was placed at the end of the chamber, at a distance of 780 mm from the FEEP emitter tip.

## III. Test No. 1

The first test campaign was aimed at giving a preliminary estimation of the main thruster parameters, i.e. onset voltage, current-voltage characteristics, beam divergence angles, beam composition, and long-term behaviour in constant and alternate polarity.

According to the current understanding of electrospray, low propellant rates promote pure ionic regime (PIR) emission and, as a consequence, low thrust and high specific impulse values. On the contrary, high propellant rates produce droplets emission and therefore higher thrust and lower specific impulse values. However, from tests it resulted that a minimum backpressure level seems to be required to have a proper propellant feeding and overcome the high impedance of the emitter channel. Indeed, the emission obtained with too low backpressure values resulted to be unstable, as the emitter current strongly decreased in time with fix applied voltage. The 5 mm propellant head used in the first test campaign (i.e., about 0.16 mbar backpressure) was evidently too small for the current emitter configuration. This was corrected in the second test campaign with a more refined propellant filling system that allowed for setting the propellant head to the preferred value within an ample range.

Typical I/V characteristics recorded in positive and negative polarity at 40 °C are shown in Fig. 8 and Fig. 9, respectively. The difference between positive and negative emission may be partially due to the fact that the I/V curves were recorded at the end of the tests, after having operated the thruster for a rather long duration in positive polarity only.

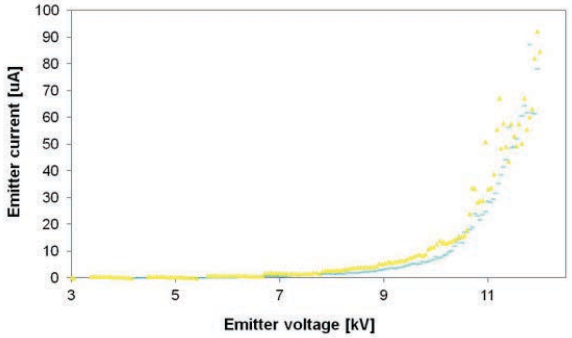


**Fig. 8 I/V curve at 40 °C, positive polarity.**

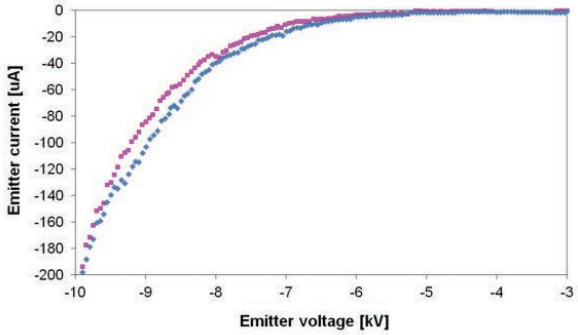


**Fig. 9 I/V curve at 40 °C, negative polarity.**

The divergency half angles obtained with the electrostatic probes resulted to be approximately 10 deg in the vertical plane and 30-40 deg in the horizontal plane. Fig. 10 shows the beam profiles at a temperature of 100 °C. The beam divergence half angles resulted to be essentially constant at varying emitter temperature, while the current drained by the probe was highly affected (the probe currents increased by a factor of 5 by increasing the emitter temperature from 20 °C to 100 °C).

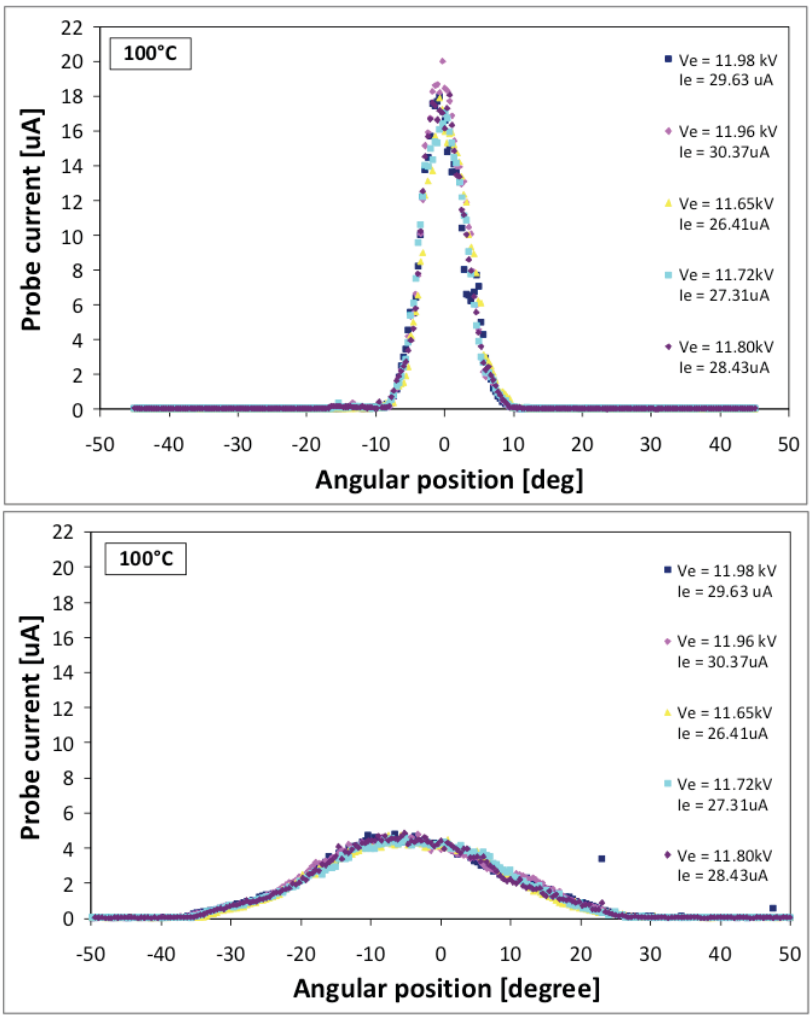


**Fig. 10 Beam profiles: in the vertical plane (above) and in the horizontal plane (below).**

During the first test campaign, ToF measurements were performed by recording the current history at the wire probe (ToF1) and at the circular target (ToF2) after abrupt cut off of the emitter voltage. The amounts of time taken by the slowest species to reach ToF1 and ToF2 are identified by the variation of slope of the voltage curves. Several data sets were recorded at emitter temeratures in the 60 °C to 120 °C range. Typical outputs of the recording oscilloscope are shown in Fig. 11.

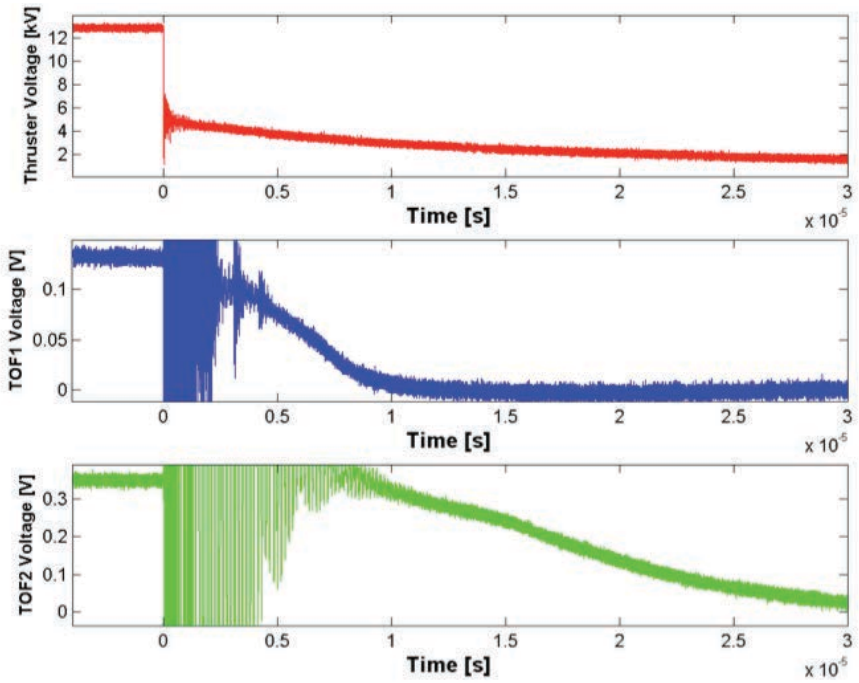


**Fig. 11 Time-of-Flight measurements. From top to bottom: emitter voltage, ToF1 voltage and ToF2 voltage (at 100 °C and emitter voltage $V_e$ = 12.9 kV)**

Table 1 summarizes the ToF measurements for the complete range of operating conditions investigated.

| Temperature [°C] | Applied voltage [kV] | Distance [m] | ToF [us] | Velocity [m/s] | m/q [kg/C] | Molecular mass [amu] |
|---|---|---|---|---|---|---|
| 60°C | 9.2 | 0.6 | 8.0 | 75,000 | $3.27 \cdot 10^{-6}$ | 313.2 |
| | | 1.3 | 18.5 | 70,270 | $3.73 \cdot 10^{-6}$ | 357.3 |
| 80°C | 12.4 | 0.6 | 6.9 | 86,956 | $3.33 \cdot 10^{-6}$ | 319.0 |
| | | 1.3 | 15.7 | 82,802 | $3.64 \cdot 10^{-6}$ | 348.7 |
| 100°C | 12.9 | 0.6 | 6.8 | 88,235 | $3.31 \cdot 10^{-6}$ | 317.4 |
| | | 1.3 | 15.4 | 84,416 | $3.62 \cdot 10^{-6}$ | 346.8 |
| 120°C | 11.5 | 0.6 | 7.5 | 80,000 | $3.59 \cdot 10^{-6}$ | 344.2 |
| | | 1.3 | 16.6 | 78,313 | $3.75 \cdot 10^{-6}$ | 359.2 |

**Table 1 Time-of-Flight data summary for 9–13 kV emitter voltage and 60–100 °C operating temperature**

Ionic compounds that are favourite candidates to be present in the beam are EMI+ (monomers), (EMI-BF4)EMI+ (dimers) and (EMI-BF4)2EMI+ (trimers). The molecular masses of these compounds are summarized in Table 2.

| Ionic compound | Molecular mass [amu] |
|---|---|
| $EMI^+$ | 111.165 |
| $(EMI\text{-}BF_4)EMI^+$ | 309.135 |
| $(EMI\text{-}BF_4)_2EMI^+$ | 507.105 |

**Table 2 Molecular masses of EMI-BF4 ionic compounds**

The dimer molecular mass of EMI-BF4 is close to that of the slowest species detected with the ToF measurements. Accordingly, the thruster beam likely contains a limited number of heavier ion clusters of droplets.

While the results of ToF tests are quite reasonable and realistic, several issues emerged related to conditioning of the output signal, because of the very low magnitude of the beam current. Using commercial op-amps to amplify the signal did not improve the signal strength to comfortable values. Better quality of the data collected was obtained with the thruster operated at high temperature, as the emitted current levels were higher. However, we suspect that, in this first set of measurements, the fastest species might have gone undetected due to poor signal-to-noise ratio. This issue was solved with the setup modified for the second test campaign.

The thruster prototype was operated in constant positive polarity mode, constant negative polarity mode and alternate polarity mode. The total firing time was 532 hours; the thruster fired:

- in positive polarity mode for 210 hours,
- in negative polarity mode for 36 hours,
- in alternate polarity mode for 284 hours, with a switch frequency of 1/60 and 1/120 Hz.

Alternate polarity was only tested after about 250 hours of firing. During the emission in a given polarity, ions of the non-ejected species accumulate into the the bulk of the liquid and, given a sufficiently long time, they are attracted toward the emitter boundaries where they can react electrochemically with the emitter material. In the EMI-BF4 case, positive species react producing surface degradation, while the negative species release gas. In both cases, the propellant exhausted but not ejected tends to accumulate debris along the emitter tip.

These phenomena may be overcome by means of a suitable alternation[5] between positive and negative polarity, so that the potential difference across the double layer formed between the emitter conductive surface and the liquid is maintained below the electrochemical window limit of the EMI-BF4. We estimate that, for currents ranging from 10 to 100 μA, the time before electrochemical reactions set in is approximately 1-10 s. In the first test campaign the power supply used didn't allow for a switching frequency high enough to prevent the onset of electrochemical effects. As a consequence, the thruster was not operated in optimal conditions, degradation of the ionic liquid propellant occurred during the tests and a significant asymmetry was detected between positive and negative characteristics. In order to correct for such undesired outcome, during the second test campaign the thruster was always run in alternate polarity mode with a faster power supply.

## IV. Test No. 2

In order to ensure proper feeding and stable emission, a hydrostatic head of about 31 mm was established in the propellant feed line, corresponding to 3.7 mbar backpressure on the emitter. By doing so, it was observed that the emission stayed pretty stable at relatively high levels of emitted current over long durations. As an example, Fig. 12 shows the emitter current as a function of time over about three hours, with emitter voltage switching between -7 and +6.9 kV and voltage-on time of 1 s per half cycle.

The thruster was always operated in alternate polarity mode, except when ToF measurements were carried out. The thruster worked for a total of 467 hours always in alternate polarity with an active firing time of 213 hours. Table 3 summarizes the cycle characteristics and the total firing time accumulated during the test campaign.

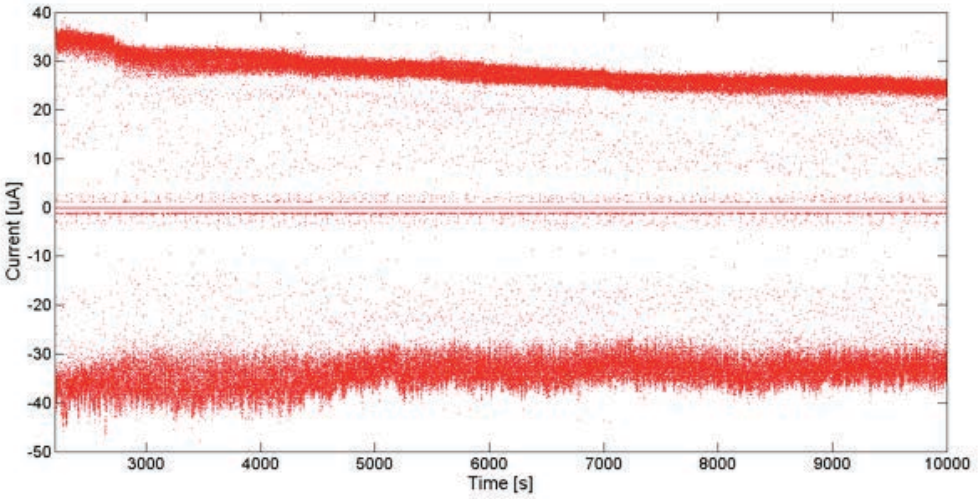


**Fig. 12 Emitter current in alternate emission (emitter voltage -7.0 kV / +6.9 kV, voltage-on time 1 s, temperature 83 °C)**

| Cycle time [ms] | Cycle number | Voltage-on time [ms] | Working time [h] | Positive firing time [h] | Negative firing time [h] | Total firing time [h] |
|---|---|---|---|---|---|---|
| 2200 | 219571 | 50<br>200 | 134.2 | 6.7 | 6.7 | 13.3 |
| 3800 | 54383 | 1000 | 57.5 | 15.0 | 14.9 | 30.0 |
| 10400 | 733 | 4000 | 2.1 | 0.8 | 0.8 | 1.6 |
| 12000 | 14939 | 4000 | 49.8 | 16.6 | 16.6 | 33.2 |
| 12800 | 140800 | 4000 | 213.1 | 66.6 | 66.6 | 133.2 |
| 16000 | 1437 | 1000<br>1500<br>4000 | 6.4 | 0.8 | 0.9 | 1.7 |
| 16900 | 842 | 1000 | 4.0 | 0.1 | 0.2 | 0.3 |
| | | **Total** | **467.0** | **106.6** | **106.7** | **213.3** |

**Table 3 Alternate polarity cycles and firing time summary**

During the second test campaign the beam scan system was not used because the thruster always fired in alternate polarity. However, an indirect measurement of the horizontal beam divergence half-angle ($\beta$) could be obtained by visual inspection of the trace left by the beam on the target (Fig. 13). The horizontal beam divergence half-angle ($\beta$) is $\beta = \text{atan}[l/(2d)]$, where $l$ is the trace width and $d$ is the emitter-target distance. Since the width $l$ is 330 mm and the distance $d$ is about 780 mm, the $\beta$ angle is close to 12 deg, confirming the value obtained in the first test campaign.

During this second test campaign, the high sensitivity MCP detector was used to perform ToF readout. This, together with the enhanced and stable current output from the thruster, resulted in high quality data sets. ToF measurements were taken setting different time scales at the oscilloscope in order to "zoom in" on the appropriate temporal regions needed to detect fast species (ions) in either positive or negative mode, or to detect slow aggregates (droplets). All ToF measurements were carried out at a temperature of 27°C.

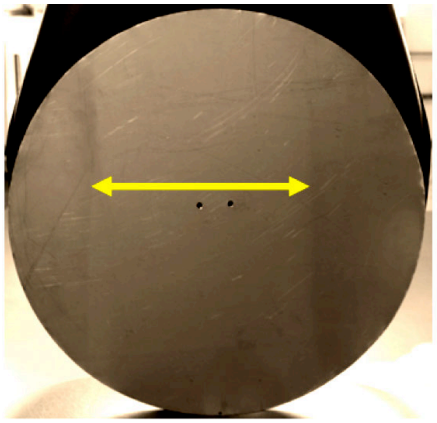

**Fig. 13 Beam footprint on the metallic target**

Figure 14 shows an example of the ToF output with the time scale properly set to detect ions in positive polarity mode.

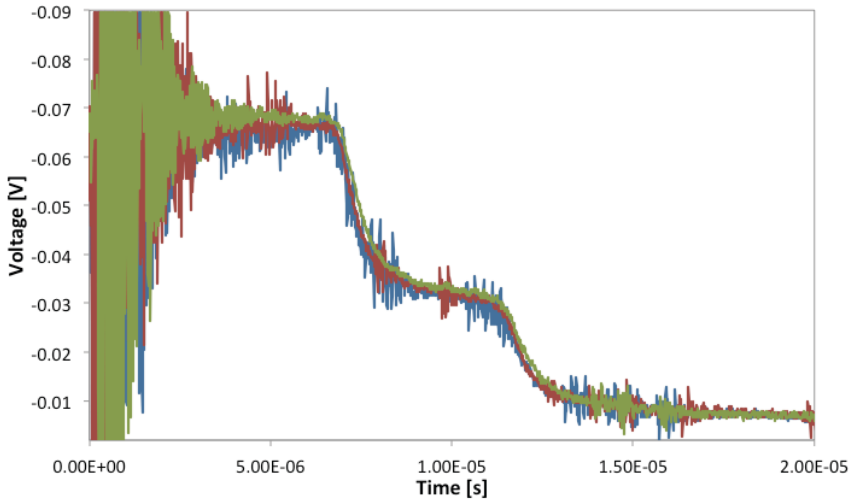


**Fig. 14 ToF measurements in positive polarity (+7.8 kV, 27°C)**

Slope variations observed in the voltage plots are related with positive monomers and dimers whose masses are 111.16 and 309.12, respectively. Table 4 summarizes the theoretical time of flight of monomers and dimers computed with the voltages used for the measurements. Experimental values of ToF match reasonably well the computed ones.

| Voltage [kV] | Monomer ToF [s] | Dimer ToF [s] |
|---|---|---|
| 7.2 | 6.98 E-6 | 11.63 E-6 |
| 7.4 | 6.88 E-6 | 11.48 E-6 |
| 7.6 | 6.79 E-6 | 11.32 E-6 |
| 7.8 | 6.70 E-6 | 11.18 E-6 |

**Table 4 Theoretical ToF for monomers and dimers in positive polarity.**

A similar set of data is shown in Fig. 15 for ions in negative polarity.

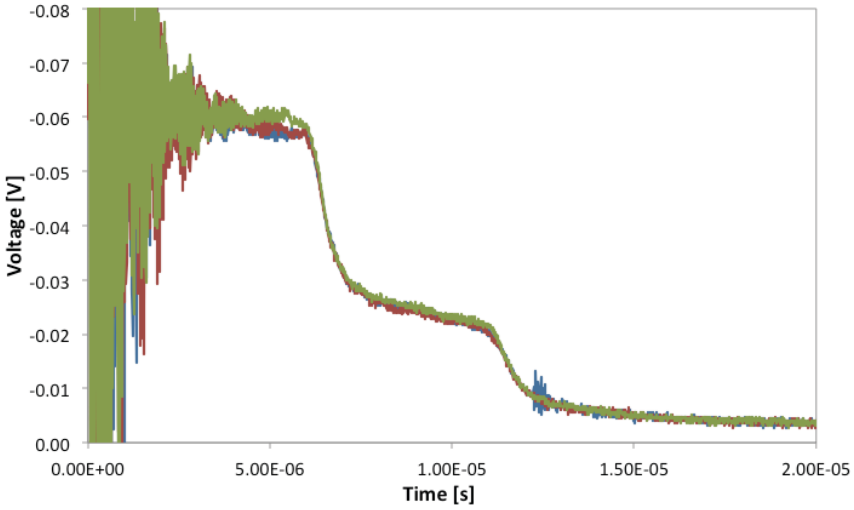


**Fig. 15 ToF measurements in negative polarity (-7.6 kV, 27°C)**

Slope variations observed in the voltage plots are related with negative monomers and dimers whose masses are 86.805 and 284.77, respectively. Table 5 summarizes the theoretical time of flight of monomers and dimers computed with the voltages used for the measurements. Again, experimental values of ToF match reasonably well the computed ones.

| Voltage [kV] | Monomer ToF [s] | Dimer ToF [s] |
|---|---|---|
| 6.2 | 7.52 E-6 | 12.54 E-6 |
| 6.9 | 7.13 E-6 | 11.88 E-6 |
| 7.2 | 6.98 E-6 | 11.63 E-6 |
| 7.4 | 6.88 E-6 | 11.48 E-6 |

**Table 5 Theoretical ToF for monomers and dimers in negative polarity.**

Fig. 16 shows the ToF data with the time scale properly set to detect slow species (droplets) in positive polarity mode with +6.9 kV. A close-up of the data (Fig. 17) reveals the slope change.

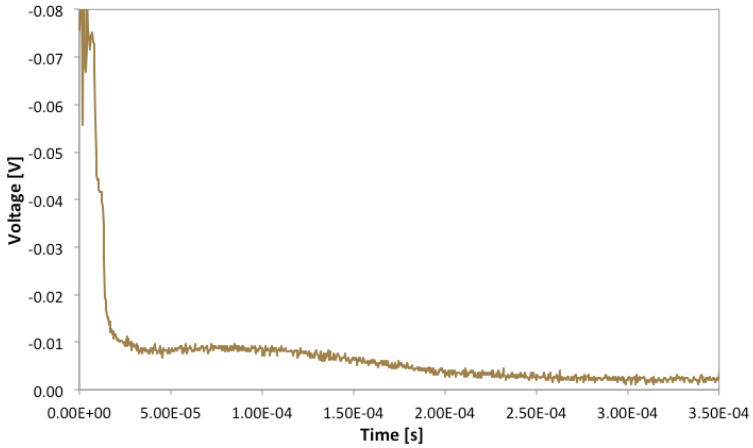


**Fig. 16 TOF measurement for detecting slow species (6.9 kV, 27°C).**

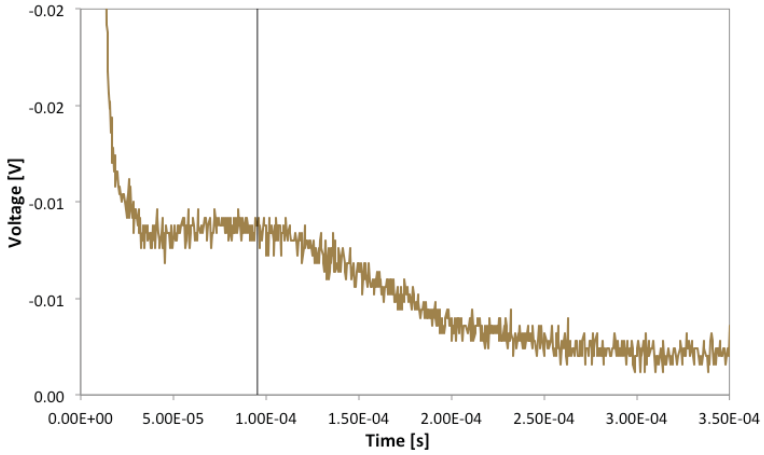


**Fig. 17 Close-up of the slow species ToF data.**

From such data, the velocity of the slowest species is $v$ = 0.78 m / $9.5 \cdot 10^{-5}$ s = 8210 m/s. The corresponding mass-to-charge ratio is $m/q = 2.05 \cdot 10^{-4}$ kg/C. Assuming only singly charged species, the molecular mass is $M$ = 197.6, so that the number of molecules in a single droplet is approximately equal to 99.8.

Similar results were obtained with measurements carried out by varying the acceleration voltage between 6 and 8 kV, both in positive and negative polarity mode. The results show that the beam is mainly composed of monomers and dimers, but also of a spectrum of droplets, whose heaviest one is made up of about 100 EMI-BF4 molecules.

From the relative contribution of monomers, dimers and droplets to the ToF output, average data can be extracted for the contribution of the different species to the total current collected at the detector. As an example, Fig. 18 and Table 6 show the results for a voltage of 7.2 kV.

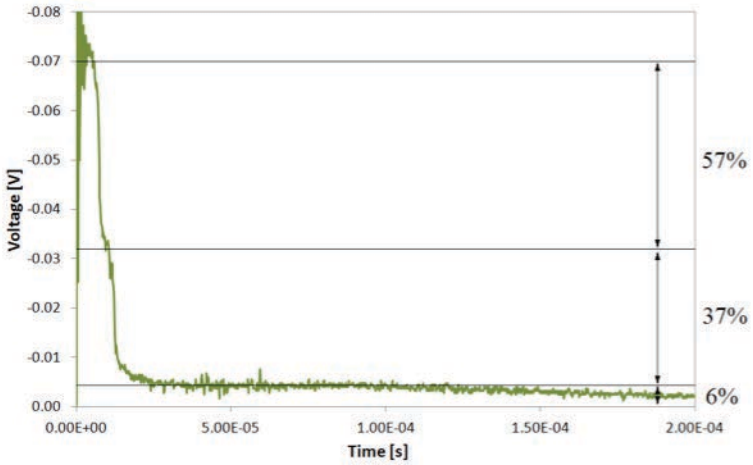


**Fig. 18 ToF output contribution of beam species (7.2 kV, 27°C)**

| | Distance [m] | Molecular mass [amu] | Velocity [m/s] | Time [s] | Current fraction |
|---|---|---|---|---|---|
| $(EMI)^+$<br>$(BF_4)^-$ | 0.78 | 111.16<br>86.805 | 111,798.9<br>126,514.3 | 6.98E-6<br>6.17E-6 | 0.541 |
| $(EMI\text{-}BF_4)(EMI)^+$<br>$(EMI\text{-}BF_4)\ (BF_4)^-$ | 0.78 | 309.125<br>284.77 | 67,041.7<br>69,849.7 | 1.16E-5<br>1.12E-5 | 0.368 |
| 100 $(EMI\text{-}BF_4)\ (EMI)^+$<br>100 $(EMI\text{-}BF_4)\ (BF_4)^-$ | 0.78 | ~ 19,900 | ~ 8,350 | ~ 9.34E-5 | 0.091 |

**Table 6 Average data for 7.2 kV ToF measurements**

Having evaluated the beam current fraction, we can now compute the mass flow rate of the each beam species as:

$$\dot{m}_i = \sum_i \frac{\alpha_i I}{\frac{q}{m_i}}$$

where $I$ is the beam current, $\alpha_i$ and $m_i$ are the beam current fraction and the mass of the $i$-th species, and $q$ is the elementary charge. Therefore, total mass flow rate and thrust are:

$$\dot{m}_{\mathrm{tot}} = \sum_i \dot{m}_i$$

$$T = \sum_i \dot{m}_i v_{\mathrm{i}}$$

where $\dot{m}_i$ and $v_i$ are the mass flow rate and the velocity of the $i$-th species. The specific impulse is

$$I_{sp} = \frac{T}{g_0 \dot{m}_{\mathrm{i}}}$$

where $g_0$ is the Earth gravity acceleration. In the above formulas, summations are to be extended to all species composing the beam. Using ToF our data, the index $i$ takes the values 1, 2 and 3 to identify monomers, dimers and droplets (with N=100 EMI-BF4 molecules), respectively. Table 7 and Table 8 summarize the results for a range of operating conditions for positive and negative emitter voltage polarity, respectively. While the $\alpha_i$ coefficients of the beam current contributions vary with the current emission (a larger contribution of droplets seems to be present in the beam at low emission currents), data in Table 7 and Table 8 were computed using average values ($\alpha_1$ = 56%, $\alpha_2$ = 37%, $\alpha_3$ = 7%). Specific impulse values resulting from these computations are underestimated, as the contributions of droplets of different sizes, of which undoubtedly exists a whole spectrum, have been entirely attributed to the larger and slower aggregate.

| Emitter Temperature [°C] | Emitter Voltage [kV] | Beam current [uA] | Mass flow [mg/s] | Thrust [µN] | $I_{sp}$ [s] |
|---|---|---|---|---|---|
| 110 | 8.2 | 180 | 2.93E-03 | 52.3 | 1821 |
| | 7.5 | 70 | 1.14E-03 | 19.5 | 1741 |
| | 6.9 | 50 | 8.14E-04 | 13.3 | 1670 |
| 83 | 6.0 | 25 | 4.07E-04 | 6.2 | 1557 |
| 70 | 6.7 | 30 | 4.88E-04 | 7.9 | 1646 |
| 60 | 6.4 | 18 | 2.93E-04 | 4.6 | 1608 |
| 27 | 6.7 | 15 | 2.44E-04 | 3.9 | 1646 |

**Table 7 Summary of thruster estimated performance in positive polarity**

| Emitter Temperature [°C] | Emitter Voltage [kV] | Beam current [uA] | Mass flow [mg/s] | Thrust [µN] | $I_{sp}$ [s] |
|---|---|---|---|---|---|
| 110 | 8.4 | 200 | 3.20E-03 | 56.3 | 1792 |
| | 7.6 | 85 | 1.36E-03 | 22.8 | 1704 |
| | 6.9 | 60 | 9.61E-04 | 15.3 | 1624 |
| 83 | 6.2 | 30 | 4.81E-04 | 7.3 | 1539 |
| 70 | 6.9 | 40 | 6.41E-04 | 10.2 | 1624 |
| 60 | 6.6 | 25 | 4.01E-04 | 6.2 | 1588 |
| 27 | 6.7 | 20 | 3.20E-04 | 5.0 | 1600 |

**Table 8 Summary of thruster estimated performance in negative polarity**

In order to provide an independent check on the performance figures resulting form the computations above, the change in time of the propellant hydrostatic head was monitored by visual inspection of the meniscus in the feeding duct during a sufficiently long firing time at 27°C. After 120 h of firing the level of propellant had decreased by about 3.9 mm (Fig. 19).

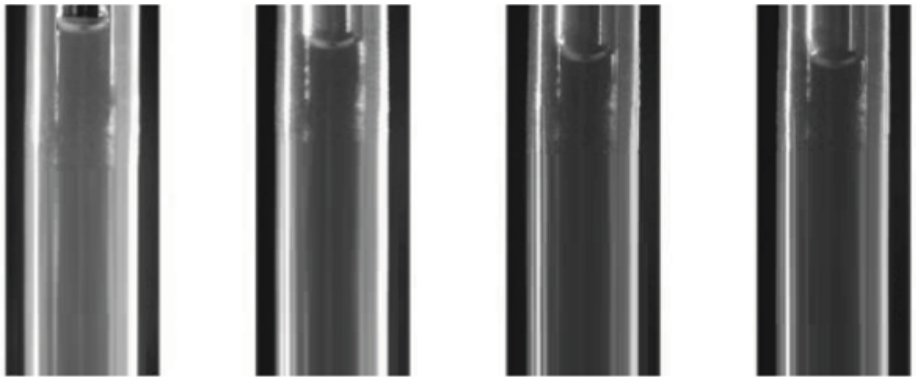

**Fig. 19 Propellant head decrease during a 120 h period of firing**

As the internal diameter of the duct is 5 mm and the EMI-BF4 density is 1218 kg/m$^3$, the actual mass consumption results to be about 96 mg. The corresponding propellant mass consumption resulting from the theoretical mass flow rates, taking into account the current and voltage levels actually recorded during the 120 h period, is about 105 mg (45.4 mg of positive ions and 59.3 mg of negative ions). The difference between the two computations is about 9%, which is considered as a very good agreement, given the various uncertainties in the visual estimate of the meniscus position and the conservative assumptions made in the specific impulse estimation via ToF results.

## V. Conclusion

The IL-FEEP performance recorded during the two test campaigns here reported is quite encouraging in view of future applications of this thruster. Stable, repeatable emission was obtained in alternate polarity. For the first time, reliable data were collected on the composition of the thruster's ejected beam, using the time-of-flight mass spectrometry technique. A conservative estimate of the specific impulse form the experimental data yields values of 1600 to 1800 s, which are well suited to the envisaged application to small satellite missions.

## Acknowledgments

Parts of this work were supported with funding from the European Commission FP7 programme E-Sail. The authors gratefully acknowledge the collaboration of Mr. Ugo Cesari of Alta's micropropulsion laboratory. Mr. Simone Perugia contributed to some of the data collection and reduction activities.

## References

[1]Paita, L., Cesari, U., Giusti, N., Priami, L., Nania, F., Rossodivita, A., Andrenucci, M., Estublier, D., "ALTA FT-150 FEEP-Overview and development status", SPC2012_2365880, Proc. Space Propulsion Conference, Bordeaux, 2012.

[2]Marcuccio, S., Pergola, P., Giusti, N., "IL-FEEP: a Simplified, Low Cost Electric Thruster for Micro- and Nano-Satellites", ESA-CNES, Proc. Small Satellites Systems and Services Symposium 2012, June 4-8 2012, Portorose, Slovenia.

[3]Marcuccio, S., Giusti, N., Pergola, P., "Development of a Miniaturized Electric Propulsion System for the E-Sail Project", 62nd International Astronautical Federation Congress, Cape Town, South Africa, IAC-11-B4-6A-3-x11311, October 2011.

[4]Marcuccio, S., Giusti, N., Pergola, P., "Ionic Liquid FEEP: Recent Experimental Results", 63rd International Astronautical Congress, Naples, Italy, IAC-12-A1-8-15, October 2012.

[5]Lozano P., Martínez-Sánchez M., "Ionic liquid ion sources: suppression of electrochemical reactions using voltage alternation", *Journal of Colloid and Interface Science* 280, 149–154, 2004.